VOL. 20, NO. 2-2, 2021, 25-29
www.elektrika.utm.my
ISSN 0128-4428

ELEKTRIKA
Journal of Electrical Engineering

Influence of Leg Geometry on the Performance of Bismuth Telluride-based Thermoelectric Generator

Md. Nazibul Hasan and **Mohamed Sultan Mohamed Ali***

School of Electrical Engineering, Faculty of Engineering, Universiti Teknologi Malaysia,
81310 UTM Johor Bahru, Johor, Malaysia

*Corresponding author: sultan_ali@fke.utm.my

Abstract: Thermoelectric generators have been widely used to transform heat into electrical energy. Over the last few decades, researchers have studied the impact of thermoelement height and cross-section area on the efficiency of thermoelectric generators. This paper investigates and analyzes the effect of various thermoelement leg geometries, including rectangular, trapezoidal, cylindrical and cone, for a bismuth telluride-based thermoelectric generator using finite element analysis. The influence of thermoelement leg height on achieving an optimized temperature gradient, producing open-circuit voltage, and achieving maximum output power is studied. Based on the analysis, the thermoelectric generator with the cone shaped leg provided optimal temperature gradient, the open-circuit voltage of 87.8 mV and a maximum power of ~270 mW at a leg height of 5 mm.

Keywords: Bismuth telluride, Finite element analysis, Thermoelectric generators, Thermoelement.

Article History: received 25 May 2021; accepted 12 June 2021; published 15 September 2021.

1. INTRODUCTION

Growing energy consumption demand and escalating concern about environmental degradation have piqued researcher's interest in the development of efficient and renewable energy technologies. These technologies have enormous potential for transforming various ambient energy sources, such as solar radiation, heat, and mechanical vibration, into electrical energy. This implies the ultimate solution for a continuous supply of renewable energy without causing ecological detriment [1, 2]. Among the renewable technologies, thermoelectric generators have been used in a variety of devices due to their remarkable advantages, such as versatility to different temperature ranges, instantaneous energy conversion without any transitional stage, high reliability, long-term stability, longevity, and noiseless operation [3, 4]. With the continued advancement of portable and wearable electronic devices, thermoelectric generators have emerged as an enticing energy source that can serve as an extension of a battery or as the sole power source for long-term operations. Despite its rapid development, thermoelectric generator's low conversion efficiency and maximum output power (P_0) prevent them from finding pervasive use in practical applications.

Several studies were carried out while developing a highly efficient thermoelectric generator module, which can be classified into three types. The properties of thermoelectric materials used in thermoelectric generators have been adjusted in the first category. Since the performance of thermoelectric material is determined by its dimensionless figure-of-merit (ZT), $ZT = S^2\sigma T/\kappa_t$, where S, σ, T, and κ_t are the Seebeck coefficient, electrical conductivity, absolute temperature, and total thermal conductivity, respectively. Thus, P_0 and efficiency have been improved by optimizing the values of S, σ, T, and κ_t [5]. Various materials have been applied at different temperature levels. For instance, at near-room temperatures, bismuth telluride (Bi_2Te_3) and its alloys have considered being the most efficient materials and have been extensively used [6, 7]. While, materials such as lead telluride (PbTe) [8], lead-free tin selenide [9], copper selenide [10] and magnesium antimonide [11] are considered under medium-temperature materials. Silicon-germanium alloys, on the other hand, are notable high-temperature thermoelectric materials [12].

The second category includes segmented and cascaded thermoelectric generators. In comparison to conventional thermoelectric generators, both types of generators have substantially elevated P_0 and conversion efficiency. For example, Hadjistassou et al. numerically investigated the performance of the Bi_2Te_3-PbTe incorporated segmented thermoelectric generator and obtained a peak efficiency of 5.29 % for a temperature gradient (ΔT) of 324.6 K [13], while Kanimba et al. showed P_0 of 51 W with an efficiency of 10.2% at a ΔT of 500 K for three-stage cascaded skutterudite-PbTe based thermoelectric generator [14]. The third research category focused on optimizing the geometrical shape of thermoelements in thermoelectric generators to improve overall generator efficiency by lowering electrical resistance and increasing thermal resistance. For instance, Wang et al. achieved a P_0 of 7.6 W

and efficiency of 15.3 % at ΔT of 500 K by varying the height and cross-sectional area of PbTe-based thermoelements in a thermoelectric generator [15]. In another report, Yu et al. investigated the effect of module geometry on power generation performance and realized an enhanced power density by 4.5 times through geometric modification [16].

The aim of this study is to design a three-dimensional thermoelectric generator module utilizing *n*-type and *p*-type Bi_2Te_3 thermoelements and to investigates the effect of thermoelement leg geometries on obtaining the optimal ΔT, open-circuit voltage (V_{oc}) and P_0 using finite element analysis. Thermoelements have been modeled and evaluated in this regard with various leg geometries including rectangular, trapezoidal, cylindrical and cone. The remainder of this paper is organized as follows: Section 2 discusses the conceptual diagram and governing equations of a thermoelectric generator. Section 3 discusses and analyzes the main findings while utilizing the geometric structures. Finally, the paper concludes with key outcomes.

2. THERMOELECTRIC GENERATOR DESIGN

A thermoelectric generator is a solid-state energy transducer that can transform ΔT into electrical energy via the Seebeck effect [17, 18]. Figure 1 depicts the conceptual design of the proposed thermoelectric generator with different thermoelement leg geometries, including rectangular, trapezoidal, cylindrical and cone. All the thermoelement pairs are made up of *n*-type Te-Bi_2Te_3 [21] and *p*-type $Bi_{0.5}Sb_{1.5}Te_3$ [22]. The *n*- and *p*-type thermoelements are electrically connected in series and thermally coupled in parallel, and they are connected to silver electrodes. When one side of the thermoelement is exposed to the hot side temperature (T_h) and the other side is held at room temperature (T_c), ΔT is formed across the thermoelements. Consequently, the majority of the charge carriers, such as holes and electrons formed by *p*-type and *n*-type thermoelements, respectively, transfer from higher to lower concentration [23-26]. V_{oc} generated by a pair of *n* and *p*-type thermoelements can be expressed as:

$$V_{oc} = nS_{pn}(T_h - T_c) = nS_{pn}\Delta T \tag{1}$$

where *n* is the number of thermoelement pairs, S_{pn} is the Seebeck coefficient between *p*-and *n*-type thermoelements, where S_p is positive for *p*-type and S_n is negative for *n*-type thermoelements. Internal resistance (R_{in}) is a crucial factor for a thermoelectric generator since it affects the voltage and power generation. The resistance offered by the thermoelements and followed by electrodes can be determined by the following equation:

$$R = n(R_{p,n} + R_{Ag}) = \frac{h}{\sigma A} \tag{2}$$

where *n* is the number of thermoelement pairs, σ and A define the electrical conductivity and area of the *p*- and *n*-type thermoelements as well as electrodes, respectively.

Under matched-load conditions, P_0 can be expressed as:

$$P_0 = \frac{V_{oc}^2}{4R_l} = \frac{n^2 S_{pn}^2 \Delta T^2 \sigma A}{4h} \tag{3}$$

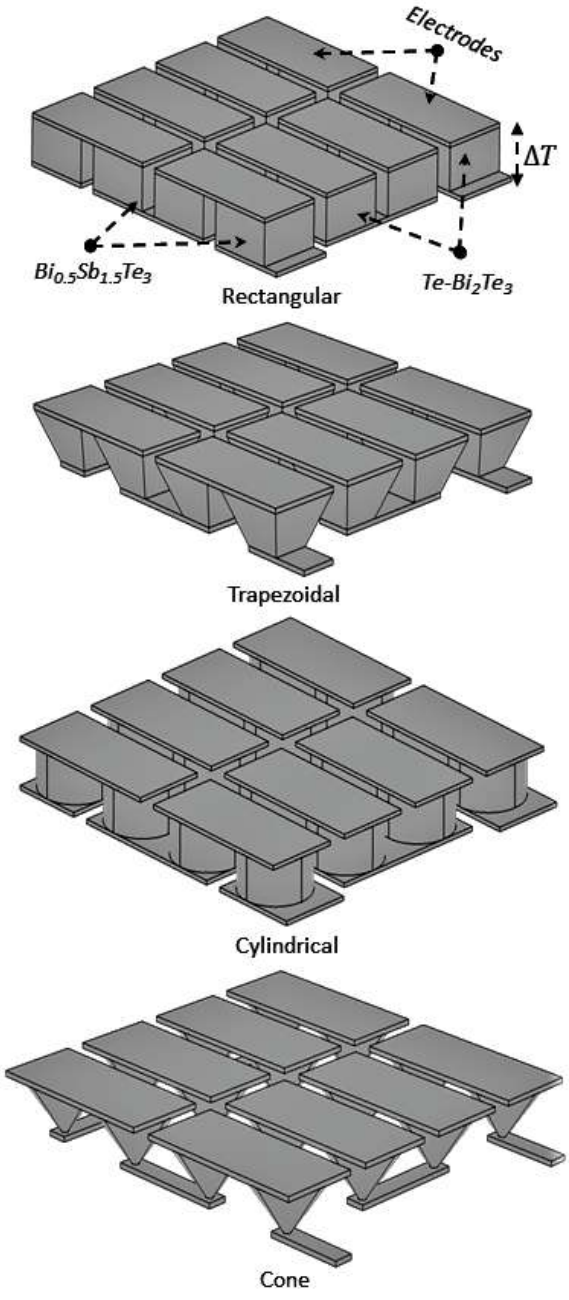

Figure 1. Thermoelectric generator with different geometries of thermoelement legs.

where R_l is the load resistance. Equation (4) can be used to describe the heat transfer rate (Q) and heat flux (q) via thermoelement.

$$q = \frac{Q}{A} = \kappa \frac{\Delta T}{h} \tag{4}$$

2.1 Finite Element Analysis

COMSOL Multiphysics® was used to perform finite element analysis simulation. In thermoelectric analysis, heat energy conversion can be described as [19]:

$$\left(\rho.C_p u.\frac{\partial T}{\partial t}+\nabla.q\right)=Q+Q_{ted} \tag{5}$$

where ρ, C_p, u, T and Q_{ted} define density, specific heat capacity at constant stress, the velocity vector of translational motion, absolute temperature, thermoelastic damping per unit volume. Energy conservation can be described as:

$$\left\{\nabla\left(\kappa.\nabla T\right)-T.J.\frac{\partial S}{\partial T}.T+\rho.J\right\}=0 \tag{6}$$

where J is the current density. The electric charge and temperature distributions are stable at steady-state conditions. The following are some of the other significant equations used in the AC/DC module during the simulation phase:

$$\nabla.J=0 \tag{7}$$

$$E=-\nabla.V \tag{8}$$

$$J=\sigma.\left(E-S.\nabla T\right) \tag{9}$$

where E defines the electrical field. Solving these equations on a finite element mesh for ΔT and V_{oc} yielded the temperature and potential distribution.

The study is carried out with the following assumptions to simplify the assessment of the heat transfer mechanism in this model.

- Thermoelectric generator is regarded as being in a steady state.
- On the top surface of the thermoelectric generator module, a heat source with a constant temperature T_h of 348.5 K is used. Other surfaces are thermally insulated.
- Both electrical and thermal contact resistances of the thermoelectric generator module are neglected.
- The temperature has no impact on the material properties of *p*-type and *n*-type thermoelements.

3. RESULTS AND DISCUSSION

The following sections present the simulation results and analysis of the proposed thermoelectric generator. The effect of thermoelement leg geometries to achieve the optimal ΔT, V_{oc} and P_0 is investigated in this section.

3.1 Optimal Temperature Gradient and Open-Circuit Voltage

The aim here is to investigate the effect of temperature distribution through various leg geometry such as rectangular, trapezoidal, cylindrical, and cone to attain the optimum ΔT and V_{oc} while varying the height of the thermoelements. Figure 2 depicts the temperature distribution through the various leg geometry when a T_h of 348.5 K is applied to the top of the thermoelements. As the height of the thermoelements increases while the area of the thermoelements remains constant at 2 mm × 2 mm, the thermal resistance of the thermoelements increases, resulting in a higher ΔT around the thermoelements and, as a result, an increased V_{oc}. Figure 3 displays the simulated results of the heat distribution through various leg

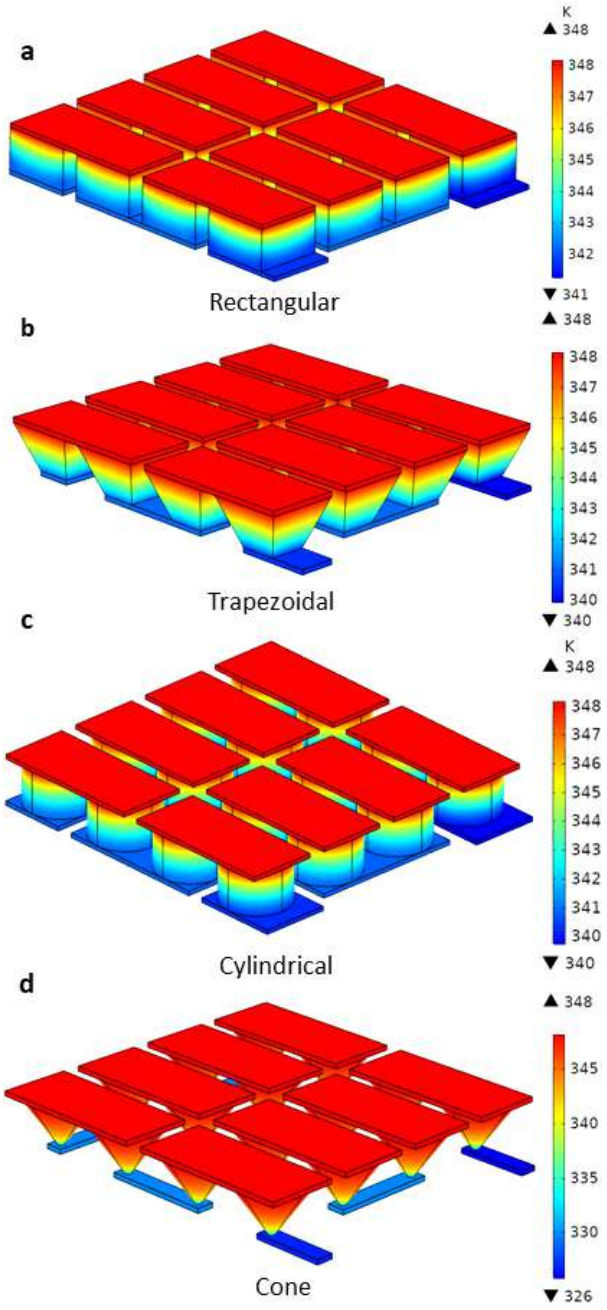

Figure 2. Finite element analysis results showing temperature distribution through the (a) rectangular, (b) trapezoidal, (c) cylindrical and (d) cone legs of the thermoelectric generator module.

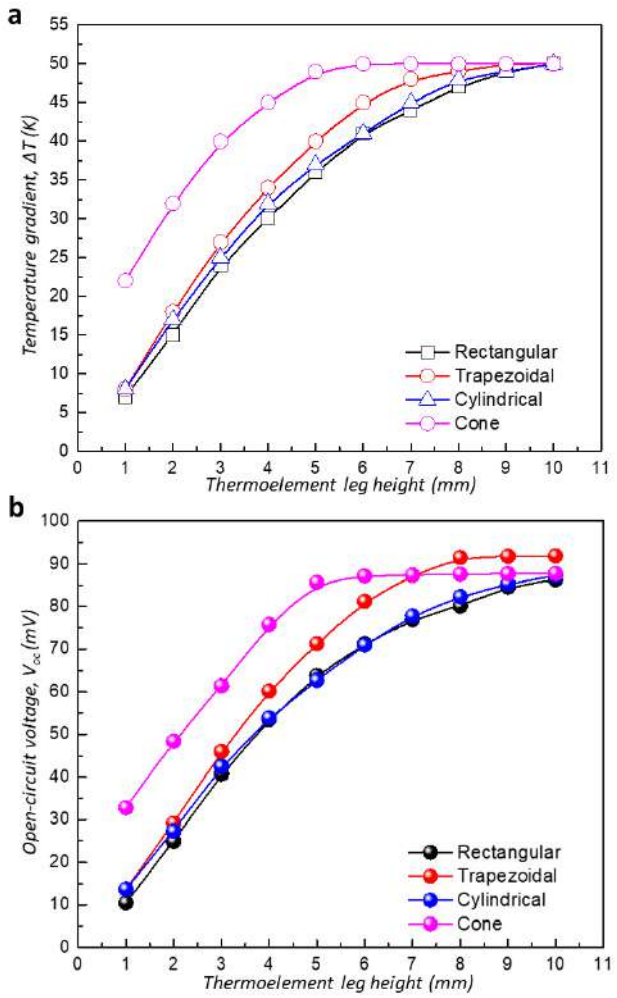

Figure 3. Effect of thermoelement leg height on (a) temperature gradient and (b) open-circuit voltage.

geometry of the proposed thermoelectric generator module with optimal thermoelements height. Except for the cone, which showed slightly different temperature decays than the other legs, all other geometry showed fairly similar and linear temperature profile changes. This result is due to the different cross-sectional areas of the cone legs. Based on the simulation, an optimum ΔT of 50 K was obtained for cone legs at thermoelements height of 5 mm, while the highest V_{oc} of 91.9 mV was obtained for the trapezoidal leg at thermoelements height of 8 mm.

3.2 Influence of Leg Geometry on Maximum Power

Figure 4 depicts the maximum electric power as a function of thermoelements leg height and leg geometries. It can be seen that P_0 for each sort of thermoelement leg increases initially with increasing leg height before reaching maximum power at an optimal height, and then begins to decrease with increasing thermoelement leg height. The results clearly show that a thermoelectric generator must be designed with a particular thermoelement leg geometry with the optimal leg height in order to achieve maximum P_0. Based on the simulation, a maximum P_0 of ~270 mW was obtained for cone legs at a height of 5 mm.

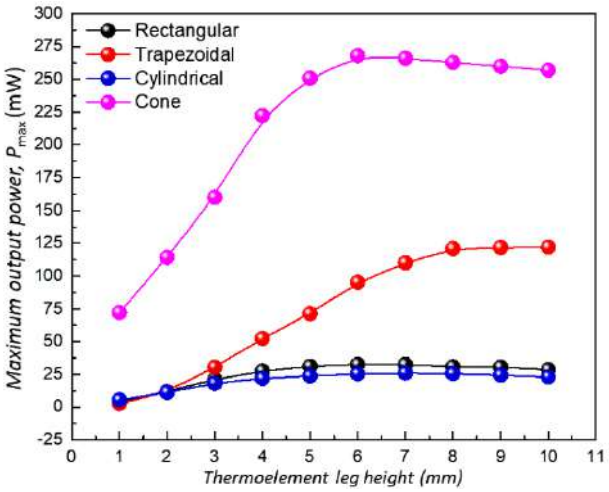

Figure 4. Influence of thermoelement leg height on maximum power.

4. CONCLUSION

The dependence of thermoelectric performance on the thermoelements leg with four different geometry was investigated using finite element analysis. The effect of thermoelement leg length on ΔT, V_{oc} and P_0 was investigated for a Bi_2Te_3-incorporated thermoelectric generator module. As per the results of the analysis, leg geometry has a significant impact on heat distribution. The rectangular, trapezoidal, and cylindrical legs geometry with varying heights resulted in nearly linear temperature profile changes, whereas the cone leg had slightly different temperature decays due to its different cross-sectional areas. The change in leg height has a significant impact on the internal resistance and thermal conductance for each leg geometry, and thus generated divergent power. The thermoelectric generator with cone leg geometry showed a maximum P_0 of ~270 mW at a leg height of 5 mm. The novel structure and findings could help to develop an efficient thermoelectric generator for diverse practical applications.

ACKNOWLEDGMENT

This work was supported by the Ministry of Education Malaysia through Fundamental Research Grant Scheme (Grant No. FRGS/1/2018/TK04/UTM/02/5). Mohamed Sultan thank the Universiti Teknologi Malaysia for Industry-International Incentive Grant (IIIG Q.J130000.3651.03M03) and Altec Industrial & Engineering Supply Sdn Bhd for Contract Research Grant (R.J130000.7651.4C371).

REFERENCES

[1] A. Khalil, A. Elhassnaoui, S. Yadir, O. Abdellatif, Y. Errami, and S. Sahnoun, "Performance comparison of TEGs for diverse variable leg geometry with the same leg volume," *Energy,* vol. 224, p. 119967, 2021.

[2] D. Ji *et al.*, "Geometry optimization of solar thermoelectric generator under different operating conditions via Taguchi method," *Energy Conversion and Management,* vol. 238, p. 114158, 2021.

[3] M. N. Hasan, H. A. Rahim, M. A. Ahmad, and M. S. M. Ali, "Modelling and simulation of magnesium antimonide based thermoelectric generator," *Indonesian Journal of Electrical Engineering and Computer Science,* vol. 19, no. 2, pp. 686-692, 2020.

[4] M. N. Hasan, S. Sahlan, K. Osman, and M. S. Mohamed Ali, "Energy Harvesters for Wearable Electronics and Biomedical Devices," *Advanced Materials Technologies,* p. 2000771.

[5] M. N. Hasan, H. Wahid, N. Nayan, and M. S. Mohamed Ali, "Inorganic thermoelectric materials: A review," *International Journal of Energy Research,* vol. 44, no. 8, pp. 6170-6222, 2020.

[6] S. I. Kim *et al.*, "Dense dislocation arrays embedded in grain boundaries for high-performance bulk thermoelectrics," *Science,* vol. 348, no. 6230, pp. 109-114, 2015.

[7] Y. Yu *et al.*, "Simultaneous optimization of electrical and thermal transport properties of $Bi_{0.5}Sb_{1.5}Te_3$ thermoelectric alloy by twin boundary engineering," *Nano Energy,* vol. 37, pp. 203-213, 2017.

[8] G. Tan *et al.*, "Non-equilibrium processing leads to record high thermoelectric figure of merit in PbTe-SrTe," *Nature communications,* vol. 7, no. 1, pp. 1-9, 2016.

[9] L.-D. Zhao *et al.*, "Ultralow thermal conductivity and high thermoelectric figure of merit in SnSe crystals," *Nature,* vol. 508, no. 7496, pp. 373-377, 2014.

[10] K. Zhao *et al.*, "Ultrahigh thermoelectric performance in $Cu_{2-y}Se_{0.5}S_{0.5}$ liquid-like materials," *Materials Today Physics,* vol. 1, pp. 14-23, 2017.

[11] F. Meng, S. Sun, J. Ma, C. Chronister, J. He, and W. Li, "Anisotropic thermoelectric figure-of-merit in Mg_3Sb_2," *Materials Today Physics,* vol. 13, p. 100217, 2020.

[12] Y. Peng *et al.*, "Realizing high thermoelectric performance in *p*-type $Si_{1-x-y}Ge_xSn_y$ thin films at ambient temperature by Sn modulation doping," *Applied Physics Letters,* vol. 117, no. 5, p. 053903, 2020.

[13] C. Hadjistassou, E. Kyriakides, and J. Georgiou, "Designing high efficiency segmented thermoelectric generators," *Energy conversion and management,* vol. 66, pp. 165-172, 2013.

[14] E. Kanimba, M. Pearson, J. Sharp, D. Stokes, S. Priya, and Z. Tian, "A modeling comparison between a two-stage and three-stage cascaded thermoelectric generator," *Journal of Power Sources,* vol. 365, pp. 266-272, 2017.

[15] X. Wang *et al.*, "Geometric structural design for lead tellurium thermoelectric power generation application," *Renewable Energy,* vol. 141, pp. 88-95, 2019.

[16] C. Yu, S. Zheng, Y. Deng, C. Su, and Y. Wang, "Performance Analysis of the Automotive TEG with Respect to the Geometry of the Modules," *Journal of Electronic Materials,* vol. 46, no. 5, pp. 2886-2893, 2017.

[17] K. V. Selvan, M. N. Hasan, and M. S. Mohamed Ali, "Methodological reviews and analyses on the emerging research trends and progresses of thermoelectric generators," *International Journal of Energy Research,* vol. 43, no. 1, pp. 113-140, 2019.

[18] K. V. Selvan, M. N. Hasan, and M. S. M. Ali, "State-of-the-art reviews and analyses of emerging research findings and achievements of thermoelectric materials over the past years," *Journal of Electronic Materials,* vol. 48, no. 2, pp. 745-777, 2019.

[19] S. Shittu, G. Li, X. Zhao, X. Ma, Y. G. Akhlaghi, and E. Ayodele, "High performance and thermal stress analysis of a segmented annular thermoelectric generator," *Energy Conversion and Management,* vol. 184, pp. 180-193, 2019.